Korean J. Chem. Eng., 36(4), 620-624 (2019)
DOI: 10.1007/s11814-019-0248-4

pISSN: 0256-1115
eISSN: 1975-7220

Electrochemical characteristics of lithium-excess cathode material ($Li_{1+x}Ni_{0.9}Co_{0.05}Ti_{0.05}O_2$) for lithium-ion batteries

Hyoung Shin Ko*, Hyun Woo Park, Geun Joong Kim**, and Jong Dae Lee**,†**

*New Material R&D Center, Huayou New Energy Technology Co., Ltd., No. 18, Wuzhen E. Rd., Economic Development Zone of Tonxiang, Zhejiang Province, 314500, China
**Department of Chemical Engineering, Chungbuk National University, 1 Chungdaero, Seowongu, Cheongju, Chungbuk 28644, Korea
(*Received 2 December 2018 • accepted 21 February 2019*)

Abstract−A $Ni_{0.9}Co_{0.05}Ti_{0.05}(OH)_2$ precursor was synthesized with the concentration gradient method. To overcome the Li-ion shortage the problem due to the formation of a solid electrolyte interphase (SEI) layer during the initial charge/discharge process in the cathode material, lithium-excess $Li_{1+x}Ni_{0.9}Co_{0.05}Ti_{0.05}O_2$ ($0 \le x \le 0.07$) cathode materials were investigated by physical and electrochemical analyses. The physical properties of the lithium-excess cathode materials were analyzed using FE-SEM and XRD. A coin type half-cell was fabricated with the electrolyte of 1 M $LiPF_6$ dissolved in organic solvents (EC : EMC=1 : 2 vol%). The electrochemical performances were analyzed by the initial charge/discharge efficiency, cycle stability, rate performance and electrochemical impedance spectroscopy (EIS). The initial charge capacity of the cathode material was excellent at about 199.8-201.7 mAh/g when the Li/Metal ratio was 1.03-1.07. Additionally, the efficiency of the 6.0 C/0.1 C was 79.2-79.9%. When the Li/Metal ratio was 1.05, the capacity retention showed the highest stability of 97.8% after 50 cycles.

Keywords: Lithium-excess, Li/Metal Ratio, Li-ion Shortage, SEI Layer, Cathode Material

INTRODUCTION

Lithium-ion batteries (LIBs) are being developed for portable electronic devices, such as notebooks, cellular phones and smart watches as well as electric vehicles (EVs) and energy storage systems (ESSs), which require LIBs with a high capacity and energy density. As the demand for EVs and ESSs increases, LIBs need to be technologically advanced with the following features: miniaturization, lightweight and a fast/rapid charge/discharge. In addition, many studies have been conducted to satisfy the high energy density, cycle stability and safety requirements of LIBs [1,2].

$LiCoO_2$ is most widely used as a cathode material in which the lithium-ions are reversibly intercalated and deintercalated; moreover, it is easy to synthesize and has an excellent cycle performance [3]. However, $LiCoO_2$ is very expensive because of a major component of cobalt (Co), which is a limited resource. When charging and discharging are repeated in a high voltage range, the lithium ions can be intercalated and deintercalated. However, the electrochemical performance deteriorates due to structural changes at the high voltage range, and the actual usable capacity at the operating voltage is about half of the theoretical capacity. To overcome the disadvantages of the $LiCoO_2$, other cathode materials are required. As an alternative to $LiCoO_2$ with its high cost and structural problems, many studies have replaced Co with other transition metals such as nickel (Ni) and manganese (Mn). As a substitute for $LiCoO_2$, $LiNiO_2$ has attracted much attention due to its high capacity and low cost [4]. However, $LiNiO_2$ has some problems, making its commercialization difficult. The nickel ions present in the lithium layer cause a cation mixing phenomenon, which deteriorates the cycle performance. During charging, Ni^{2+} is oxidized to Ni^{3+} causing a change in the crystal structure, which results in a decrease in the performance of the battery. To overcome the problems of $LiNiO_2$, cathode materials have been studied by replacing Ni with Co, Mn, Al, and Ti [5-7]. Cathode materials made by partial substitution of the Ni with Ti, such as $LiNi_{1-x}Ti_xO_2$, can maintain both electron neutrality and structural stability. Recently, titanium was substituted into a high nickel content cathode material such as $LiNi_{0.8-y}Ti_yCo_{0.2}O_2$ and $LiNi_{0.7}Co_{0.2}Ti_{0.05}Mg_{0.05}O_2$ to improve the cycle stability, structural and thermal stability and electrochemical properties [8,9]. When the Li-ion content in the cathode material is reduced, the cation mixing and Jahn-Teller effects increase. Also, it is reported that the electrochemical performance deteriorates. To overcome this problem, studies have used Li-rich cathode materials such as $Li(Li_{0.17}Ni_{0.25}Mn_{0.58})O_2$, and $Li[Li_{0.2}Ni_{0.18}Co_{0.03}Mn_{0.58}]O_2$ [10-12].

In this study, cathode materials were synthesized by varying the Li/Metal ratio (1.00, 1.03, 1.05 and 1.07) to overcome Li-ion shortage due to the formation of SEI layer during the initial charge/discharge in the titanium-substituted Ni-rich cathode materials. The physical properties of the cathode materials with different Li/Metal ratios were analyzed by FE-SEM and XRD. After assembling a coin type half-cell using $LiPF_6$ (EC : EMC=1 : 2 vol%) as the electrolyte, the electrochemical properties of the lithium-excess cathode materials were investigated by the initial charge/discharge, cycle stability, rate capability and EIS.

†To whom correspondence should be addressed.
E-mail: jdlee@chungbuk.ac.kr

EXPERIMENTAL

Spherical $Ni_{0.9}Co_{0.05}Ti_{0.05}(OH)_2$ hydroxide precursors were synthesized by the co-precipitation method [13]. $NiSO_4{\cdot}6H_2O$ (Norilsk), $CoSO_4{\cdot}7H_2O$ (Sigma-Aldrich) and 24 wt% $Ti(SO_4)_2$ solution (American Elements) were used as starting materials and dissolved in distilled water. A 2.0 M solution of Ni and other metals was fed into a batch reactor (100 L) filled with a solution ion-exchanged water under a nitrogen atmosphere. NaOH solution and NH_4OH solution were also fed into the reactor as the precipitant and chelating agent, respectively. The pH value, reactive temperature and stirring speed were controlled at 10.80, 50 °C and 450 rpm, respectively. The final precursor powder was obtained by filtering, washing and drying at 110 °C for 24 h. The Li/Metal ratio was calculated from the molar concentration ratio of lithium and the transition metals. The precursor and $LiOH{\cdot}H_2O$ (FMC Co.) were mixed at 1,500 RPM in a 5 L volume multi-purpose mixer for 15 min to achieve a Li/Metal ratio of 1.00, 1.03, 1.05 and 1.07. The mixture was calcined at 760 °C for 12 h in a flow of oxygen (5 L/min) to obtain the $Li_{1+x}Ni_{0.9}Co_{0.05}Ti_{0.05}O_2$ ($0 \le x \le 0.07$) powder. The calcined material was pulverized using an air classifying mill (ACM), and then, the $Li_{1+x}Ni_{0.9}Co_{0.05}Ti_{0.05}O_2$ ($0 \le x \le 0.07$) cathode materials were prepared using a #325 mesh standard sieve. The synthesis procedure of the cathode material is shown in Fig. 1. The physical properties of the synthesized cathode material with different Li/Metal ratios were measured by X-ray diffraction (XRD; SmartLab, Rigaku) to analyze the change in crystal structure from each manufacturing condition. The surface characteristics and particle shape were analyzed by FE-SEM (Field emission scanning electron microscope, S-2500C, JEOL).

For the preparation of slurry, the active material, denka black and polyvinylidene fluoride (PVDF) were dissolved in N-methyl-2-pyrrolidone (NMP) with a weight ratio of 94 : 3 : 3. The slurry was coated uniformly onto aluminum foil with a micrometer applicator at a constant thickness of 150 μm, dried at 105 °C in a 40 torr vacuum oven for 12 hours and then rolled to a thickness of 45± 5 μm. The loading weight was 8.0±0.1 mg/cm^2, and the packing density was 2.8±0.1 g/cm^3. The anode was made of 99.9% lithium metal (Honjo Metal) with a thickness of 0.5 mm. The electrolyte was 1 M $LiPF_6$ dissolved in ethylene carbonate (EC) and ethyl methyl carbonate (EMC) (1 : 2, v/v). Additionally, a microporous trilayer membrane (Celgard 2400, Celgard) was used as a separator. The battery assembly process was in a dry room where the dew point was maintained at −60 °C or lower.

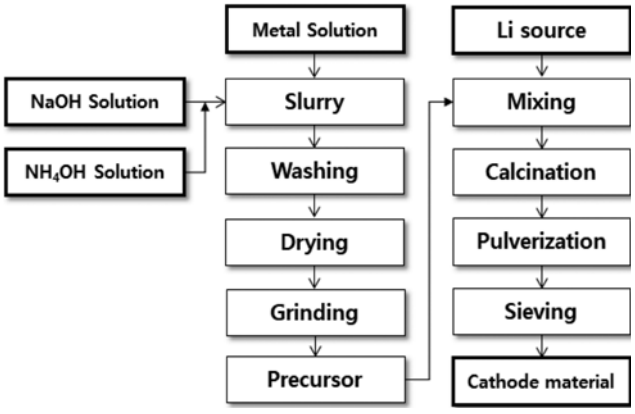

Fig. 1. Schematic diagram for the synthesis of the cathode materials.

After electrochemical activation, the battery performance was evaluated at room temperature, using a charge/discharge device (Toscat-3100, Toyo system) to analyze the initial charge/discharge, rate stability and cycle stability. To electrochemically activate the synthesized cathode materials, initial charging was performed by using the constant current/constant voltage (CC/CV) method up to 4.5 V (vs. Li/Li^+) at a 0.1 C (20 mA/g) rate. After charging in the CC method, when the voltage reached 4.5 V, it was maintained at 4.5 V, and the charging was continued to the cutoff when the current decreased to 0.01 mA. Discharging was performed with the CC method up to 3.0 V (vs. Li/Li^+) at a 0.1 C rate. The initial charge/discharge capacity was evaluated between 3.0 and 4.3 V (vs. Li/Li^+). The rate capabilities were evaluated by setting the charge rate to 0.5 C and the discharge rate from 0.1 to 6 C in the range of 3.0 and 4.3 V (vs. Li/Li^+). Cycling stability was evaluated by performing a single charge/discharge cycle at 0.1 C followed by 50 cycles of charging at 0.5 C and discharging at 1 C. EIS of the cells was conducted using ZIVE LAB MP2 (Won A Tech) before charge and discharge at frequencies from 1,000 KHz to 0.01 Hz.

RESULTS AND DISCUSSION

1. Analysis of the Physical Properties of the Lithium-excess Cathode Materials

Fig. 2 shows the SEM images of the $Li_{1+x}Ni_{0.9}Co_{0.05}Ti_{0.05}O_2$ ($0 \le x \le 0.07$) cathode materials with the different Li/Metal ratios. In the figure, all of the cathode materials retained the spherical shape of the precursor and D_{50} values between 9 and 10 μm. As a result, it was not possible to distinguish the shape change according to the change in the Li/Metal ratio using FE-SEM. The XRD pattern of a synthesized cathode material is shown in Fig. 3 using an X-ray dif-

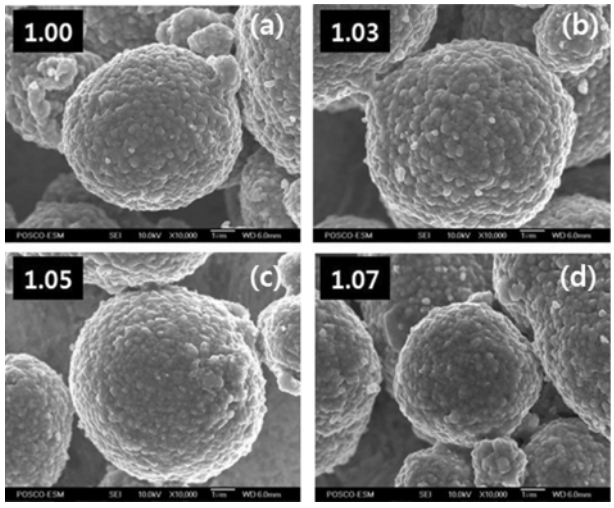

Fig. 2. FE-SEM images of $Li_{1+x}Ni_{0.9}Co_{0.05}Ti_{0.05}O_2$ ($0 \le x \le 0.07$) synthesized with various Li/Metal ratios (a) 1.00, (b) 1.03, (c) 1.05 and (d) 1.07.

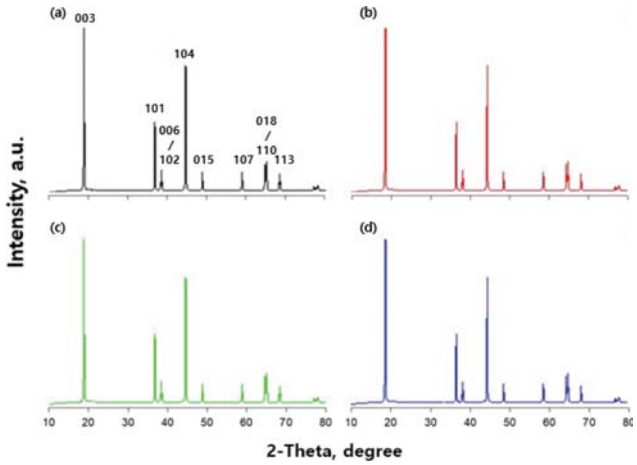

Fig. 3. (a)-(d) XRD patterns of $Li_{1+x}Ni_{0.9}Co_{0.05}Ti_{0.05}O_2$ (0≤x≤0.07) synthesized with various Li/Metal ratios (a) 1.00 (b) 1.03, (c) 1.05 and (d) 1.07.

fractometer to analyze the crystal structure and lattice constant of the synthesized cathode material. The peaks of the (006), (102), (108), and (110) planes are clearly separated, and the layered structure is well developed. The $Li_{1+x}Ni_{0.9}Co_{0.05}Ti_{0.05}O_2$ (0≤x≤0.07) cathode material with the peak of the (003), (101), (006) (102), (104), (015), (107), (018), (110) and (113) crystal plane was found to have a well-developed layered hexagonal α-$NaFeO_2$ structure with an $R\bar{3}m$ space group [14,15].

Cation mixing is known to increase the instability of the structure by causing Ni^{2+} ions to interfere with the diffusion of Li^+ ions in the charge/discharge process, thereby decreasing the electrochemical performance. According to Nagayama et al. [16], when the ratio of $I_{(003)}/I_{(104)}$ is lower than 1.3, cations located in the Li-site exhibit high cation mixing characteristics and the reversible capacity tends to decrease. The peak intensity of the (003) plane can be greatly influenced by the orientation in the measurement, and as such, the R-factor can be used to more accurately confirm the electrochemical performance. The R-factor is expressed as the value of $(I_{(102)}+I_{(006)})/I_{(101)}$, which indicates the hexagonal ordering. When the R-factor value has a value of 0.41-0.44, there is almost no cation mixing [17-19]. The unit cell refinement results from the X-ray diffraction pattern are shown in Table 1. No changes were observed for the a-axis and the c-axis and volume change of the unit cell due to changes in the Li/Metal ratio; however, the R-factor values were slightly different. The lowest R-factor was found for a Li/Metal ratio of 1.05, which indicates that hexagonal ordering is the highest and cation mixing is the lowest.

Table 1. The lattice parameters of $Li_{1+x}Ni_{0.9}Co_{0.05}Ti_{0.05}O_2$ (0≤x≤0.07) synthesized with various Li/Metal ratios

		Li/Metal ratio, M/M			
		1.00	1.03	1.05	1.07
a	Å	2.8780	2.8779	2.8777	2.8777
c	Å	14.2283	14.2280	14.2275	14.2263
c/*a*	-	4.9438	4.9439	4.9438	4.9436
Cell volume	$Å^3$	102.1	102.1	102.0	102.0
R-factor	-	0.438	0.427	0.422	0.424

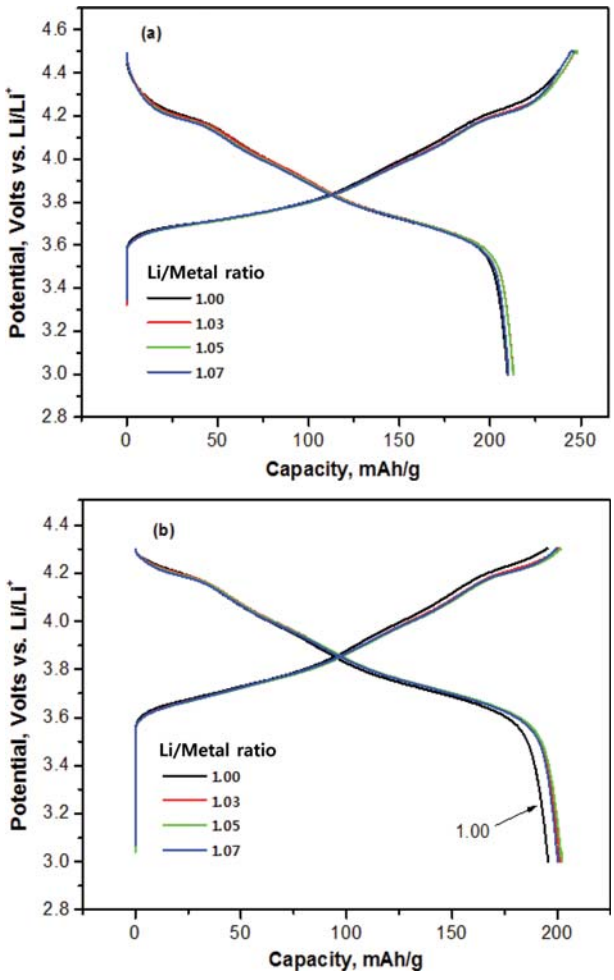

Fig. 4. Electrochemical profiles $Li_{1+x}Ni_{0.9}Co_{0.05}Ti_{0.05}O_2$ (0≤x≤0.07) synthesized with various Li/Metal ratios (a) electrochemical activation and (b) initial charge/discharge.

2. Electrochemical Characterization of the Lithium-excess Cathode Materials

The electrochemical activation and initial charge/discharge profiles of $Li_{1+x}Ni_{0.9}Co_{0.05}Ti_{0.05}O_2$ (0≤x≤0.07) are shown in Fig. 4 and Table 2. The electrochemical activation step was performed in the CC/CV mode with a cut-off voltage and charge/discharge rate of

Table 2. Electrochemical characterization results of $Li_{1+x}Ni_{0.9}Co_{0.05}Ti_{0.05}O_2$ (0≤x≤0.07) synthesized with various Li/Metal ratios

			Li/Metal ratio, M/M			
			1.00	1.03	1.05	1.07
Activation	0.1 C charge	mAh/g	246.1	248.1	247.9	245.9
	0.1 C discharge	mAh/g	209.6	212.8	212.7	210.1
	Efficiency	%	85.2	85.8	85.8	85.4
1^{st} Cycle	0.1 C charge	mAh/g	195.3	200.8	201.7	199.8
	0.1 C discharge	mAh/g	195.6	201.1	202.0	200.1
	Efficiency	%	100.2	100.1	100.1	100.2

3.0-4.5 V (vs. Li/Li^+) and 0.1 C (20 mAh/g), respectively. In Fig. 4(a), the charge capacity of the cathode material was 246-248 mAh/g; the discharge capacity was 210-213 mAh/g, and the coulombic efficiency was 85.2-85.8%. After completing the electrochemical activation, the initial charge/discharge was performed in the CC/CV mode with a cut-off voltage and charge/discharge rate of 3.0-4.3 V (vs. Li/Li^+) and 0.1 C (20 mAh/g), respectively. In Fig. 4(b), the initial charge/discharge capacities and reversal efficiency of the cathode materials were 200-202 mAh/g and 100% for three of the cathode materials, excluding the one with a Li/Metal ratio of 1.00. On the other hand, the cathode material synthesized with a Li/Metal ratio of 1.00 exhibited a relatively low charge and discharge capacity of 195.3 and 195.6 mAh/g, respectively. The reason for the low charge/discharge capacity compared with other cathode materials is that Li-ions with reversible characteristics in the initial charge/discharge process are consumed by participating in the SEI layer reaction generated on the surface of the cathode material [20]. In the second charge/discharge process, the surface reaction by the HF present in the cathode material and the electrolyte causes oxygen desorption, and the reversible capacity is reduced by a change in the surface structure [21].

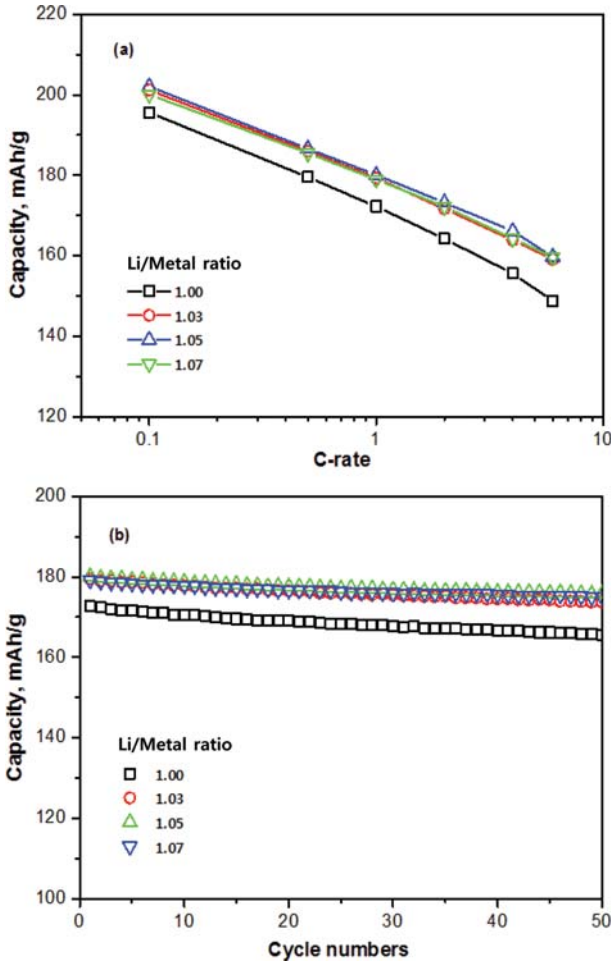

Fig. 5. Electrochemical performances of $Li_{1+x}Ni_{0.9}Co_{0.05}Ti_{0.05}O_2$ (0≤x≤0.07) synthesized with various Li/Metal ratios (a) rate and (b) cycle.

Table 3. Electrochemical performances of $Li_{1+x}Ni_{0.9}Co_{0.05}Ti_{0.05}O_2$ (0≤x≤0.07) synthesized with various Li/Metal ratios

			Li/Metal ratio, M/M			
			1.00	1.03	1.05	1.07
C-rate	0.5 C discharge	mAh/g	179.5	185.9	186.6	185.5
	1.0 C discharge	mAh/g	172.2	179.3	180.1	178.9
	2.0 C discharge	mAh/g	164.2	171.6	173.2	172.2
	4.0 C discharge	mAh/g	155.6	163.9	166.1	164.2
	6.0 C discharge	mAh/g	148.7	159.1	159.8	159.7
	6.0 C/0.1 C	%	76.1	79.2	79.2	79.9
Cycles	1^{st} discharge	mAh/g	172.6	179.4	180.1	179.2
	50^{th} discharge	mAh/g	166.2	174.2	176.2	174.9
	Retention	%	96.3	97.1	97.8	97.6

The rate and cycle profiles of the $Li_{1+x}Ni_{0.9}Co_{0.05}Ti_{0.05}O_2$ (0≤x≤0.07) are shown in Fig. 5 and Table 3. The rate capabilities of the cathode materials were determined at a fixed charge rate of 0.5 C and discharge rates of 0.1, 0.2, 0.5, 1, 2, 4, and 6 C in the range of 3.0-4.3 V (vs. Li/Li^+). As shown in Fig. 5(a), the slope of the capacity change with the increasing rate of the discharge rate for all the cathode materials showed a similar decreasing tendency; however, the discharge capacity was low for the cathode material with a Li/Metal ratio of 1.00. The retention rates of the $Li_{1+x}Ni_{0.9}Co_{0.05}Ti_{0.05}O_2$ (0≤x≤0.07) were 76.1, 79.2, 79.2 and 79.9%, respectively, and the lowest retention rate was observed for the cathode material with a Li/Metal ratio of 1.00. As a result, the reason why the discharge capacity and retention rate are low is thought to be a result of an insufficient amount of lithium ions. The hexagonal ordering increases with a decreasing R-factor when the Li/Metal ratio is 1.03-1.07 shown in Fig. 3, and the initial discharge capacity and reversibility efficiency tend to increase [22]. On the other hand, the rate characteristic is considered to be degraded because of the low crystallinity with the Li/Metal ratio of 1.00.

The cycle stability was evaluated by performing 50 charge/discharge cycles at a fixed charge and discharge rate (0.5 and 1 C, respectively). As shown in Fig. 5(b), the cathode materials had the relatively lowest cycle stability (96.3%) with a Li/Metal ratio of 1.00, while excellent cycle stability (97.1-97.8%) was observed with Li/Metal ratios of 1.03-1.07. The $Li_{1+x}Ni_{0.9}Co_{0.05}Ti_{0.05}O_2$ (0≤x≤0.07) cathode material had a lower rate capability, but exhibited much better cycle stability than $LiNi_{0.9}Co_{0.05}Mn_{0.05}O_2$ cathode material [23]. As the amount of Li-ions exhibiting reversible characteristics decreases, the crystal structure is affected as the number of charge/discharge cycles increases. As such, a change in the surface structure occurs, and the degradation of the cathode material is accelerated. Therefore, the degradation of the cathode material with a Li/Metal ratio of 1.00 is fast because the amount of Li-ions is small.

In Fig. 6, EIS of the synthesized cathode material was measured in the range of 1,000 KHz to 0.01 Hz. A semicircular shape of a high frequency region is observed, and a semicircular high frequency region shows a charge transfer resistance [24]. The semicircular resistance of synthesized $Li_{1+x}Ni_{0.9}Co_{0.05}Ti_{0.05}O_2$ (0≤x≤0.07) cathode materials shows 166 ohm, 122 ohm, 123 ohm and 118 ohm, respectively. As the lithium content in the cathode material increases, the sta-

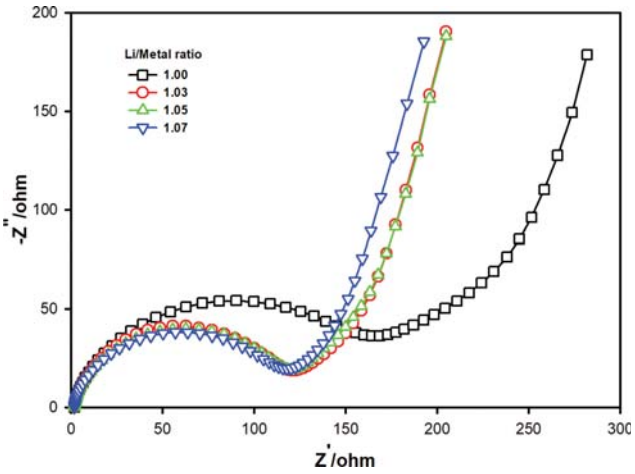

Fig. 6. Nyquist plots of $Li_{1+x}Ni_{0.9}Co_{0.05}Ti_{0.05}O_2$ ($0 \le x \le 0.07$) cathode materials.

bility of the electrode structure increases, and the lower charge-transfer resistance of the $Li_{1+x}Ni_{0.9}Co_{0.05}Ti_{0.05}O_2$ ($0.03 \le x \le 0.07$) materials than that of the $LiNi_{0.9}Co_{0.05}Ti_{0.05}O_2$ material is the reason why it has the highest rate capability [25].

CONCLUSION

Cathode materials with different Li/Metal ratios of 1.00, 1.03, 1.05 and 1.07 were synthesized using the precursor $Ni_{0.9}Co_{0.05}Ti_{0.05}(OH)_2$ prepared by the concentration gradient method. The particle size and crystal structure of the lithium-excess cathode materials for lithium ion batteries were analyzed by SEM and XRD, and electrochemical characteristics were investigated by the initial charge/discharge, cycle stability, rate capability and EIS. It was confirmed that the initial discharge capacity has a high capacity for a Li/Metal ratio range of 1.03-1.07. Considering the cycle stability, rate capability and EIS of the cathode material, the electrochemical performance was excellent for the Li/Metal ratio range of 1.03-1.07. Thus, a high Li/Metal ratio of a cathode material has a beneficial effect on the cycle stability and rate capability.

ACKNOWLEDGEMENTS

This work was supported by Korea Evaluation institute of Industrial Technology (KEIT) through the Carbon Cluster Construction project [10083621, Development of preparation technology in petroleum-based artificial graphite anode] funded by the Ministry of Trade, Industry & Energy (MOTIE, Korea).

REFERENCES

1. J. W. Fergus, *J. Power Sources*, **195**, 939 (2010).
2. A. Kraytsberg and Y. Ein-Eli, *Adv. Energy Mater.*, **2**, 922 (2012).
3. Q. Cao, H. P. Zhang, G. J. Wang, Q. Xia, Y. P. Wu and H. Q. Wu, *Electrochem. Commun.*, **9**, 1228 (2007).
4. W. Ebner, D. Fouchard and L. Xie, *Solid State Ionics*, **69**, 238 (1994).
5. E. Rossen, C. D. W. Jones and J. R. Dahn, *Solid State Ionics*, **57**, 311 (1992).
6. Q. Zhong and U. Sacken, *J. Power Sources*, **54**, 221 (1995).
7. J. Kim and K. Amine, *Electrochem. Commun.*, **3**, 52 (2001).
8. H. Liu, J. Li, Z. Zhang, Z. Gong and Y. Yang, *Electrochim. Acta*, **49**, 1151 (2004).
9. V. Subramanian and G. T. K. Fey, *Solid State Ionics*, **148**, 351 (2002).
10. P. Oh, S. Myeong, W. Cho, M. J. Lee, M. Ko, H. Y. Jeong and J. Cho, *Nano Lett.*, **14**, 5965 (2014).
11. F. Nomura, Y. Liu, T. Tanabe, N. Tamura, T. Tsuda, T. Hagiwara, T. Gunji, T. Ohsaka and F. Matsumoto, *Electrochim. Acta*, **269**, 321 (2018).
12. H. Z. Zhang, Q. Q. Qiao, G. R. Li, S. H. Ye and X. P. Gao, *J. Mater. Chem.*, **22**, 13104 (2012).
13. H. S. Ko, J. H. Kim, J. Wang and J. D. Lee, *J. Power Sources*, **372**, 107 (2017).
14. H. Xie, G. Hu, K. Du, Z. Peng and Y. Cao, *J. Alloys Compd.*, **666**, 84 (2016).
15. W. Li, J. N. Reimers and J. R. Dahn, *Phys. Rev. B*, **46**, 3236 (1992).
16. T. Ohzuku, A. Ueda and M. Nagayama, *J. Electrochem. Soc.*, **140**, 1862 (1993).
17. J. R. Dahn, U. V. Sacken and C. A. Michal, *Solid State Ionics*, **44**, 87 (1990).
18. Y. M. Choi, S. I. Pyun and S. I. Moon, *Solid State Ionics*, **89**, 43 (1996).
19. K. Wu, F. Wang, L. Gao, M. R. Li, L. Xiao, L. Zhao, S. Hu, X. Wang, Z. Xu and Q. Wu, *Electrochim. Acta*, **75**, 393 (2012).
20. X. Wei, S. Zhang, P. Yang, H. Li, S. Wang, Y. Ren, Y. Xing and J. Meng, *Int. J. Electrochem. Sci.*, **12**, 5636 (2017).
21. Y. S. Lee, W. K. Shin, A. G. Kannan, S. M. Koo and D. W. Kim, *ACS Appl. Mater. Interfaces*, **7**, 13944 (2015).
22. H. S. Ko, H. W. Park and J. D. Lee, *Korean Chem. Eng. Res.*, **56**(5), 718 (2018).
23. C. S. Yoon, M. H. Choi, B. B. Lim, E. J. Lee and Y. K. Sun, *J. Electrochem. Soc.*, **162**(14), A2483 (2015).
24. M. D. Levi, G. Salitra, B. Markovsky, H. Teller, D. Aurbach, U. Heider and L. Heider, *J. Electrochem. Soc.*, **146**(4), 1279 (1999).
25. T. Zhao, S. Chen, L. Li, X. Zhang, R. Chen, I. Belharouak, F. Wu and K. Amine, *J. Power Sources*, **228**, 206 (2013).